JOURNAL OF BACTERIOLOGY, Feb. 1993, p. 840–850
0021-9193/93/030840-11$02.00/0

Vol. 175, No. 3

Localization of the *Fusobacterium nucleatum* T18 Adhesin Activity Mediating Coaggregation with *Porphyromonas gingivalis* T22

SUSAN A. KINDER† AND STANLEY C. HOLT*

Departments of Periodontics and Microbiology, University of Texas Health Science Center at San Antonio, 7703 Floyd Curl Drive, San Antonio, Texas 78284-7894

Received 27 July 1992/Accepted 24 November 1992

Adherence of pathogenic bacteria is often an essential first step in the infectious process. The ability of bacteria to adhere to one another, or to coaggregate, may be an important factor in their ability to colonize and function as pathogens in the periodontal pocket. Previously, a strong and specific coaggregation was demonstrated between two putative periodontal pathogens, *Fusobacterium nucleatum* and *Porphyromonas gingivalis*. The interaction appeared to be mediated by a protein adhesin on the *F. nucleatum* cells and a carbohydrate receptor on the *P. gingivalis* cells. In this investigation, we have localized the adhesin activity of *F. nucleatum* T18 to the outer membrane on the basis of the ability of *F. nucleatum* T18 vesicles to coaggregate with whole cells of *P. gingivalis* T22 and the ability of the outer membrane fraction of *F. nucleatum* T18 to inhibit coaggregation between whole cells of *F. nucleatum* T18 and *P. gingivalis* T22. Proteolytic pretreatment of the *F. nucleatum* T18 outer membrane fraction resulted in a loss of coaggregation inhibition, confirming the proteinaceous nature of the adhesin. The *F. nucleatum* T18 outer membrane fraction was found to be enriched for several proteins, including a 42-kDa major outer membrane protein which appeared to be exposed on the bacterial cell surface. Fab fragments prepared from antiserum raised to the 42-kDa outer membrane protein were found to partially but specifically block coaggregation. These data support the conclusion that the 42-kDa major outer membrane protein of *F. nucleatum* T18 plays a role in mediating coaggregation with *P. gingivalis* T22.

Bacterial adherence is often an essential first step in the colonization and establishment of an infection in a susceptible host (30, 31). It is a highly specific process, allowing a bacterium to localize in a favorable ecological niche (3, 7, 26, 39). Adherence itself is thus an important virulence factor. Understanding the basis of this initial but essential interaction between a microorganism and its host should lead to the development of strategies to prevent adherence and thereby prevent infection.

The role of adherence in the ecology of the human oral cavity has been extensively studied (for reviews, see references 11 and 24). Its importance in dental caries is well documented, and an extensive literature supports the conclusion that streptococcal adherence to the host tooth surface is necessary for the initiation of a carious lesion (11, 21). In contrast, the role of bacterial adherence in the initiation of periodontal disease(s) has not been clearly demonstrated. Periodontal diseases consist of a group of inflammatory conditions, broadly classified as gingivitis and periodontitis, which have been associated with several gram-negative anaerobic and facultative microorganisms (12). Only recently has a concerted effort been made to understand the initial events that occur between putative periodontal pathogens and the surfaces that they colonize (12, 16, 17, 19, 20, 36).

Porphyromonas (*Bacteroides*) *gingivalis* has been strongly associated with periodontitis (13, 33, 40). In vitro studies have revealed that this microorganism possesses many properties that may function in vivo to neutralize host defense mechanisms and cause the destruction of host tissues (12). The association between the establishment of *P. gingivalis* in the subgingival microbiota and the onset of periodontal destruction has been demonstrated in an in vivo model of periodontitis (13). *P. gingivalis* has also been shown to preferentially adhere to other plaque microorganisms rather than to tooth or tissue surfaces (29), suggesting that interbacterial adherence may play a primary role in the colonization of this pathogen.

A pronounced and highly specific interaction between *P. gingivalis* and another gram-negative anaerobe implicated in periodontitis, *Fusobacterium nucleatum*, has been documented (16, 17). Previous studies have associated the *F. nucleatum-P. gingivalis* adherence with a protein adhesin on the *F. nucleatum* cells and a carbohydrate receptor on the *P. gingivalis* cells (16, 17). The purpose of this investigation was to localize the *F. nucleatum* T18 adhesin activity by examining cell envelope fractions for their ability to block coaggregation between *P. gingivalis* T22 and *F. nucleatum* T18 and to further analyze the cell envelope fractions to delineate specific proteins which may be involved in mediating this interbacterial adherence. The adhesin activity was localized to the outer membrane of *F. nucleatum* T18, and a 42-kDa major outer membrane protein (OMP) was implicated as an adhesin mediating the interaction with *P. gingivalis* T22.

MATERIALS AND METHODS

Bacterial strains and growth. *F. nucleatum* T18 and *P. gingivalis* T22 were isolated from the subgingival microbiota of cynomolgus monkeys and maintained and grown as described previously (16). Since previous investigations have demonstrated surface alterations of prokaryotic cells with prolonged growth in vitro (6), the cultures used in the experiments described here were passaged 10 times or fewer

* Corresponding author.
† Present address: Section of Periodontics, UCLA School of Dentistry, Los Angeles, CA 90024-1668.

in vitro. *Escherichia coli* JM109 was grown aerobically with aeration in Luria broth (28) at 37°C.

Buffers and harvesting procedures. Several Tris-based buffers were used in these studies. Coaggregation buffer (CB), used in the washing and suspension of cells for coaggregation assays, consisted of 1 mM Tris-HCl, 0.15 M NaCl, 0.1 mM anhydrous $MgCl_2$, and 0.1 mM $CaCl_2$ (pH 7.5). Storage buffer (SB), used in the storage of cells, vesicles, and cell envelope fractions, consisted of CB plus 2 mM *N*-α-*p*-tosyl-L-lysine chloromethyl ketone, 2 mM benzamidine, 2 mM phenylmethylsulfonyl fluoride, and 0.1% (wt/vol) NaN_3. Disruption buffer (DB) was used to suspend cells to be disrupted for the preparation of cell envelope fractions and consisted of SB without the NaN_3 but with 50 μg of DNase per ml, 50 μg of RNase per ml, and 1 M anhydrous $MgCl_2$.

F. nucleatum T18 and *E. coli* JM109 cells were harvested by Pellicon ultrafiltration with a 0.45-μm filter (Millipore, Bedford, Mass.). Cells used for the preparation of cell envelope fractions were washed in CB and resuspended in DB to a concentration of approximately 10^{10} cells per ml. Cells used for extrinsic radiolabeling (see below) were washed in phosphate-buffered saline (PBS: 100 mM potassium phosphate, 0.15 M NaCl [pH 7.5]) and then stored in PBS with 1% NaN_3. *F. nucleatum* T18 vesicles were isolated from the Pellicon 0.45-μm filtrate with a 300,000-molecular-weight exclusion filter (Millipore), pelleted by ultracentrifugation (100,000 × *g*, 2 h, 4°C), resuspended in SB, and stored at 4°C.

Preparation and proteolytic treatment of cell envelope fractions. *F. nucleatum* T18 and *E. coli* JM109 cultures were grown, harvested, and resuspended as described above. The cells were disrupted by at least five passes through a cold French pressure cell (SLM Instruments, Urbana, Ill.) at 17,000 lb/in^2. Whole cells and debris were removed by centrifugation (3,000 × *g*, 15 min, 4°C), and the resulting supernatant was subjected to ultracentrifugation (100,000 × *g*, 1 h, 4°C). The pellet, designated the cell envelope fraction (CEF), was washed three times, resuspended in SB, and stored at 4°C. The outer membrane fraction (OMF) was prepared by 2% (wt/vol) *N*-lauryl sarcosinate treatment of the CEF for 1 h at room temperature with agitation (10, 15). The insoluble OMF was pelleted by ultracentrifugation (as above), washed three times in CB, resuspended in SB, and stored at 4°C. Protease treatment (1 mg of protease per ml) was performed on the OMF (2.22 mg of OMF protein per ml) after two washes in CB under conditions recommended by the manufacturer (Sigma Chemical Co., St. Louis, Mo.). The treated membrane fractions were washed twice and then resuspended and stored in SB at 4°C. Protein concentrations were determined with the bicinchoninic acid assay (Pierce, Rockford, Ill.) with bovine serum albumin as a control (15).

Gel electrophoresis and Western immunoblotting. One-dimensional sodium dodecyl sulfate-polyacrylamide gel electrophoresis (SDS-PAGE) (18), with 12.5% polyacrylamide running and 4% polyacrylamide stacking gels, was used to resolve the CEFs and OMFs, with and without heating (100°C, 5 min). High- and low-molecular-weight standards (Bio-Rad, Richmond, Calif.) were included in each gel. Two-dimensional SDS-PAGE was performed to identify heat-modified proteins as described by Kennell and Holt (15). Proteins were visualized on gels stained with Coomassie brilliant blue R250 (0.025% [wt/vol]; Bio-Rad).

Cell envelope fractions were Western blotted by standard procedures (34) and incubated overnight with antibody (diluted in TBS [50 mM Tris HCl, 0.9% NaCl, pH 7.5]) raised against *F. nucleatum* T18 whole cells or the 42-kDa OMP (see immunological reagents below) for ca. 12 h, with agitation. The blots were washed four times with TBS for 10 min each and developed as described previously (36).

Radiolabeling of *F. nucleatum* T18 surface proteins and autoradiography. To identify proteins expressed on the bacterial cell surface, extrinsic radiolabeling with ^{125}I was performed by a modification of the Bolton-Hunter technique (5). Sulfosuccinimidyl-3-(4-hydroxyphenyl)propionate (2 ml of an 0.2-mg/ml solution in PBS, pH 7.2) was iodinated by incubation with 10 mCi of $Na^{125}I$ in the presence of Iodobeads (Pierce Chemical Co.). After 2 min of incubation at room temperature with stirring, 2.4 ml of 1-mg/ml phenylacetic acid was added and incubated for 20 s to bind any free ^{125}I. The reaction was terminated by removing the solution from the Iodobeads. The labeling reagent (0.55 ml) was then added to a suspension of *F. nucleatum* T18 cells (ca. 5×10^{10} cells suspended in 20 ml of PBS) and incubated for 20 min at 4°C with stirring. The labeled reaction was terminated by the addition of lysine (20 mg in 5 ml). The cells were pelleted (10,000 × *g*, 15 min, 4°C), washed in CB, and resuspended in DB for isolation of the cell envelope. Autoradiography was used to detect surface-exposed OMPs from one- or two-dimensional SDS-PAGE gels of the *F. nucleatum* T18 OMF prepared from ^{125}I-labeled cells (15).

Immunological reagents. (i) Antigen isolation and antibody preparation. The presumptive 42-kDa OMP adhesin was isolated by H_2O extraction of a single band from SDS-PAGE gels of the heated *F. nucleatum* T18 OMF, and purity was confirmed by SDS-PAGE. Antibody was generated to both whole cells of *F. nucleatum* T18 and the isolated 42-kDa OMP in New Zealand White rabbits as described by Weinberg and Holt (35). Immunoglobulin-enriched ammonium sulfate cuts (ASC) were prepared from the antisera by precipitation with 30 to 40% (wt/vol) ammonium sulfate, and the precipitated fraction was dialyzed extensively (36). An enzyme-linked immunosorbent assay (ELISA) (9) with whole cells of *F. nucleatum* T18 was used to assess antibody titers.

(ii) Isolation of IgG and Fab fragments. Immunoglobulin G (IgG) and Fab fragments were purified from the ASC of the antisera described above. IgG was purified with the Immunopure (A/G) IgG Purification kit (Pierce). Isolated IgG was equilibrated with CB for the coaggregation assays or with PBS for preparation of Fab fragments with the Immunopure Fab Preparation Kit (Pierce). Purified Fab fragments were concentrated and equilibrated with CB by using a Centricon-10 microconcentrator (10,000-molecular-weight cutoff; Amicon), and the purity of the IgG and Fab fragments was confirmed by SDS-PAGE (data not shown). The purified IgG and Fab fragments were diluted to a starting concentration of 1 mg of protein per ml for use in the coaggregation assays. At this concentration, the ELISA titers of the preimmune IgG ranged from 1:40 to 1:320; the titers for the *F. nucleatum* T18 whole-cell-specific IgG and 42-kDa OMP-specific IgG were 1:20,480 and 1:10,240, respectively.

Electron microscopy. Transmission and scanning electron microscopy of coaggregates were carried out as described previously (16). Vesicle and membrane fractions were prepared for negative staining by allowing a drop of the preparation to settle on a Formvar-coated grid for 10 s, and then the excess fluid was drawn off. The grids were stained with 1% (wt/vol) phosphotungstic acid (pH 7.2) for 30 s to 1 min; excess stain was removed, and the grids were air dried. *F. nucleatum* T18 cells used in immunogold labeling were fixed and dehydrated as described above, omitting the OsO_4

fixation, and embedded in LR gold (23). The specimens were sectioned and then stained by the immunocytochemical staining procedure of Berryman and Rodewald (4). The grids were stained with uranyl acetate-lead citrate (27) and air dried. Examination by transmission electron microscopy was done as described previously (16).

Coaggregation assay. The microcoaggregation assay of Kinder and Holt (16) was used to quantitate coaggregation between *P. gingivalis* T22 and either *F. nucleatum* T18 whole cells or vesicles. The inhibitory activity of *F. nucleatum* T18 cell envelope fractions or antibody preparations was examined by incorporating these preparations into the assay system at various concentrations of protein. The relative percent coaggregation was determined as the ratio of the percent coaggregation with potential inhibitors to the percent coaggregation in the absence of potential inhibitors. The percent inhibition was calculated as 100% − relative percent coaggregation. Statistical analyses consisted of a two-sample *t* test with means and standard deviation (SD).

RESULTS

Coaggregation of *P. gingivalis* T22 with whole cells and vesicles of *F. nucleatum* T18. The percent coaggregation of whole cells of *P. gingivalis* T22 with *F. nucleatum* T18 averaged 84.9% ± 9.3%. While the level of coaggregation varied with each cell batch (range of 96.7 to 53.9%), there did not appear to be a correlation between the level of coaggregation and the cellular growth phase (e.g., logarithmic versus stationary phase) or the number of in vitro passages of the cultures (data not shown).

Vesicles are membranous structures thought to result from the budding of a portion of the outer membrane of gram-negative bacteria (22). Vesicles were isolated from *F. nucleatum* T18 and examined for their ability to coaggregate with whole cells of *P. gingivalis* T22. The *F. nucleatum* T18 vesicle preparation consisted primarily of spherical structures, with few large membrane fragments and no whole cells observed in the preparation (Fig. 1A, inset). The diameter of most of the vesicles was approximately 0.05 μm, but the range was from 0.03 to 0.3 μm. The *F. nucleatum* T18 vesicles effectively coaggregated whole cells of *P. gingivalis* T22 (Fig. 1); the extent of coaggregation depended on the protein concentration. Vesicles at protein concentrations of 500, 50, and 5 μg/ml resulted in 87.9, 80.9, and 60% coaggregation, respectively. Vesicles were also produced by *P. gingivalis* T22, but few vesicles remained in the cell preparations because of the method of harvesting cells (see Materials and Methods). Thus, *P. gingivalis* T22 vesicles do not appear to have contributed to the coaggregation observed. Thin sections of the *P. gingivalis* T22 cell-*F. nucleatum* T18 vesicle coaggregates (Fig. 1A) demonstrated a close association of the vesicles with the outer membrane of the *P. gingivalis* cells. The vesicles were randomly distributed over the *P. gingivalis* surface and were often seen interposed between *P. gingivalis* cells (Fig. 1A, arrows) but also displayed a tendency to self-aggregate. Note in Fig. 1A that the large *P. gingivalis* T22 aggregate appears to be held together by both groups of *F. nucleatum* T18 vesicles and thin fibrous material emerging from the *P. gingivalis* surface. Scanning electron microscopy revealed large *F. nucleatum* T18 vesicle-*P. gingivalis* T22 cell coaggregates (Fig. 1B, inset), which formed a "woven" pattern (Fig. 1B) very similar to that seen in whole-cell *F. nucleatum* T18-*P. gingivalis* T22 coaggregates (16).

Localization of *F. nucleatum* T18 adhesin activity. The *F. nucleatum* T18 adhesin activity was localized to the OMF (Fig. 2) on the basis of the ability of this fraction to selectively interfere with the coaggregation of *F. nucleatum* T18 and *P. gingivalis* T22 whole cells. Since whole cells of *E. coli* JM109 showed little to no coaggregation with either *F. nucleatum* T18 or *P. gingivalis* T22 cells, *E. coli* JM109 CEF and OMF were used as controls. As shown in Fig. 2, the CEF from *F. nucleatum* T18 demonstrated background levels of coaggregation inhibition, as judged from the lack of difference between the coaggregation inhibition of *F. nucleatum* T18 and *E. coli* JM109 CEFs. The *F. nucleatum* T18 OMF was better able to inhibit coaggregation (82.2% inhibition at 500 μg/ml) than the *F. nucleatum* T18 CEF (41.1% at 500 μg/ml). Furthermore, this level of inhibition was significantly greater than that seen with the *E. coli* JM109 OMF (25.5% inhibition at 500 μg/ml). The *E. coli* JM109 OMF control was of particular importance, since the OMFs were prepared by extraction with *N*-lauryl sarcosinate, and the detergent alone inhibits coaggregation at concentrations of 0.05% or greater (data not shown). Therefore, it appears that the putative adhesin on *F. nucleatum* T18 is localized in the OMF, since the inhibitory activity of the OMF does not appear to be the result of the incorporation of a nonspecific protein or of residual detergent in the preparation.

The localization of the *F. nucleatum* T18 adhesin activity to the OMF was further supported by the ability of the *F. nucleatum* T18 OMF to directly coaggregate whole cells of *P. gingivalis* T22 (Fig. 3). In scanning electron micrographs, the *F. nucleatum* OMF (Fig. 3B, arrows) had the appearance of small spherical or oblong structures which were distinguished from the *P. gingivalis* cells (Fig. 3C) by their size difference. The *F. nucleatum* OMF fragments attached to the *P. gingivalis* cells with no specific orientation or position (Fig. 3A and B) and were morphologically identical to other gram-negative outer membrane fragments (22). The apparent attachment of the membrane fragments to *P. gingivalis* cells is consistent with their ability to mediate coaggregation.

Effect of proteolytic treatment on coaggregation inhibition of *F. nucleatum* T18 OMF. Data from our laboratory (16) and others (17) have implicated a protein on the surface of *F. nucleatum* as the putative adhesin mediating coaggregation with *P. gingivalis*, but no studies have documented the effect on coaggregation properties of selected proteolytic treatment of membrane fractions. The *F. nucleatum* T18 OMF was treated with several proteases, and the impact on coaggregation inhibition is shown in Fig. 4. The untreated OMF had a significant inhibitory effect on *F. nucleatum-P. gingivalis* coaggregation, resulting in 91.9, 56.9, and 2.2% inhibition of coaggregation at 500, 50, and 5 μg of protein per ml, respectively. The *E. coli* JM109 OMF, which does not appear to possess the *F. nucleatum* adhesin, demonstrated substantially less coaggregation inhibition (22.5 and 0.9% inhibition at 500 and 50 μg of protein per ml, respectively) than the *F. nucleatum* T18 OMF. Proteolytic treatment of the *F. nucleatum* T18 OMF for either 1 or 12 h at 37°C with pronase, proteinase K, or pepsin resulted in a significant decrease in the coaggregation inhibition by the OMF (Fig. 4). Incubation of the *F. nucleatum* OMF for 1 h with pronase resulted in 54.1 and 23.9% inhibition at 500 and 50 μg of protein per ml, respectively; proteinase K-treated OMF inhibited coaggregation by 45.7 and 25.2% at 500 and 50 μg of protein per ml, respectively. Incubation for 12 h with at least 1 mg of pronase, proteinase K, or pepsin per ml resulted in a reduction of coaggregation inhibition of the OMF at 500 μg/ml to 8.9, 2.8, and 21.4%, respectively. Trypsin- and papain-treated OMFs also demonstrated less

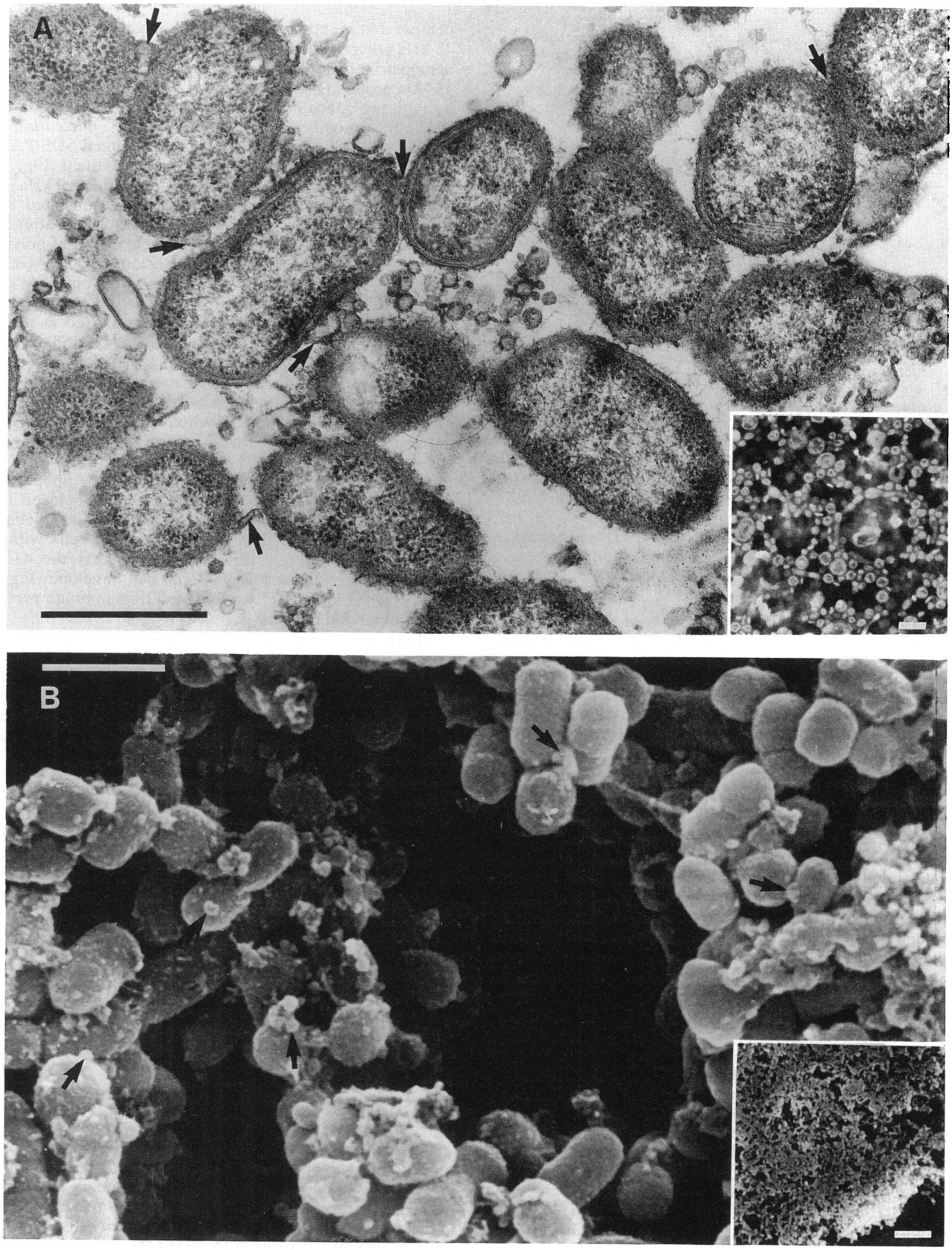

FIG. 1. Electron microscopy of coaggregates of *F. nucleatum* T18 vesicles with *P. gingivalis* T22 whole cells. (A) Thin section through coaggregate; arrows indicate vesicles interposed between whole cells of *P. gingivalis* T22. Bar, 0.5 μm. Inset: negative stain of *F. nucleatum* T18 vesicles. Bar, 0.1 μm. (B) Scanning micrograph of a coaggregate at high magnification; arrows indicate vesicle structures. Bar, 1 μm. Inset: coaggregate at low magnification. Bar, 10 μm.

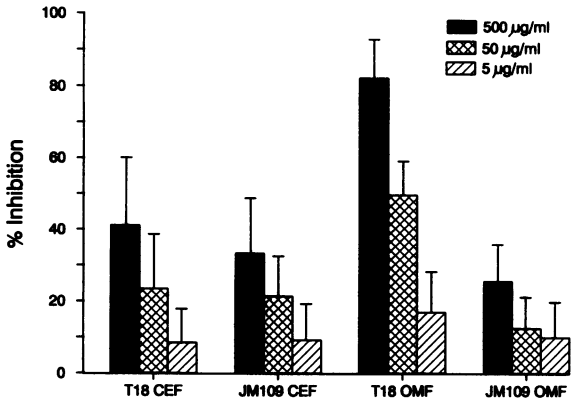

FIG. 2. Inhibition of coaggregation by *F. nucleatum* T18 CEF and OMF. Data are given as the mean percent inhibition, based on the percent coaggregation of whole cells without addition of CEF or OMF (control); the SD is indicated by the bar. The data for the CEF are the means of six experiments (each in triplicate), with a percent coaggregation for the whole cells of 79.08% ± 4.49%. The data for OMF are the means of 13 experiments (each in triplicate), with a percent coaggregation for the whole cells of 76.02% ± 7.00%. Protein concentrations were determined as described in Materials and Methods. *F. nucleatum* T18 OMF versus *E. coli* JM109 OMF at 50 and 500 μg/ml, $P < 0.05$.

inhibition than the untreated OMF, but the differences were not statistically significant (Fig. 4).

Electrophoretic and antigenic analysis of membrane fractions. The distribution of polypeptides within the *F. nucleatum* T18 CEF and OMF is shown in Fig. 5. SDS-PAGE analysis of both unheated and heated CEF revealed at least 36 major polypeptides. Comparison of the heated (100°C, 5 min) with the unheated sample indicated the presence of several heat-modified proteins, including the appearance of a major heat-modified protein at 42 kDa in the heated sample. SDS-PAGE analysis of the heated Sarkosyl-insoluble OMF, which was enriched for OMPs, revealed a selective enrichment of several polypeptides, including ones at >200, 166, 158, 85, 42, and 37 kDa, compared with the CEF. Among these proteins, the 42- and 37-kDa polypeptide levels were significantly increased, while that of a polypeptide at 85 kDa appeared to be quantitatively diminished in the heated sample (compare OMF-UH and OMF-H in Fig. 5). Other proteins were selectively lost from the CEF by treatment with Sarkosyl (Fig. 5, arrows).

Surface radiolabeling of intact *F. nucleatum* T18 cells with ^{125}I and subsequent analysis of the OMF revealed at least 10 major polypeptides that were exposed on the bacterial cell surface. These included heavily labeled polypeptides at >200, 85, 42, 39, 37, and 23 kDa (Fig. 5, OMF-UH-A and OMF-H-A), of which those at >200, 85, 42, and 37 kDa were heat modified. Antigenic studies were performed with antibody raised against *F. nucleatum* T18 whole cells and the 42-kDa major OMP. Western blots of the *F. nucleatum* T18 OMF probed with the *F. nucleatum* T18 whole-cell antibody or the 42-kDa OMP antibody are shown in Fig. 6. When the *F. nucleatum* T18 whole-cell antibody was used to probe the unheated *F. nucleatum* T18 OMF (Fig. 6, anti-WC-UH), reactivity was demonstrated to a doublet at >106 kDa as well as to polypeptides of 85, 78, 62, 42 and 39 kDa. The ladder pattern seen in Fig. 6 (anti-WC, lanes UH and H) was very similar to the distribution of lipopolysaccharide preparations. While the heated OMF (Fig. 6, anti-WC-H) showed comparable reactivity, an increase in the reactivity to the 42-kDa polypeptide was evident. The 42-kDa OMP antibody demonstrated a clear reactivity with the heat-denatured 42-kDa protein (Fig. 6, anti-42-H) but essentially no reactivity with the unheated protein (Fig. 6, anti-42-UH).

The heat-modified polypeptides of the *F. nucleatum* T18 OMF were also examined by two-dimensional SDS-PAGE, and seven heat-modified proteins were identified (Fig. 7A). At least four polypeptides of 39, 85, 158, and >200 kDa (Fig. 7A, a, b, c, and d, respectively) in the unheated state migrated to a relative molecular mass of 42 kDa after heat treatment. Therefore, the higher-molecular-weight polypeptides seen in the unheated one-dimensional SDS-PAGE are likely to be multimers of 42-kDa protein subunits. At least three other polypeptides were found to be heat modified under the conditions used. Polypeptides shifted in relative molecular mass from unheated to heated at 45 to 55, 33 to 37, and 29 to 32 kDa (Fig. 7A, e, f, and g, respectively). All of the proteins migrating at 42 kDa after heat treatment were surface exposed, as judged from ^{125}I autoradiography (Fig. 7B). The *F. nucleatum* T18 whole-cell and 42-kDa OMP antibodies clearly reacted with each of the 42-kDa polypeptides (Fig. 7C and D). The *F. nucleatum* T18 whole-cell antibody also reacted with what appears to be lipopolysaccharide, seen primarily as repeating bands displaced from the diagonal (Fig. 7C, small arrows). Immunogold labeling of thin sections from *F. nucleatum* T18 whole cells with the 42-kDa OMP antibody further indicated that the 42-kDa OMP was localized to the bacterial cell envelope (Fig. 8). The properties of the *F. nucleatum* T18 membrane proteins are summarized in Table 1.

Effect of IgG and Fab fragments on coaggregation. The possible role of the 42-kDa OMP of *F. nucleatum* T18 in coaggregation with *P. gingivalis* T22 was examined by using purified IgG and Fab fragments prepared from polyclonal antisera. ELISA titers (16) against *F. nucleatum* T18 whole cells of the preimmune ASC ranged from 1:32 to 1:512, versus titers of the whole-cell ASC of 1:65,536 and of the 42-kDa OMP ASC of 1:16,384 to 1:32,768. Purified IgG from the immune sera resulted in aggregation of the *F. nucleatum* T18 cells, most likely because of the bivalent nature of the antibody molecule, and was not of use in assessing coaggregation inhibition (data not shown). In contrast, Fab fragments isolated from the purified IgG did not aggregate the *F. nucleatum* T18 cells but did significantly inhibit *F. nucleatum* T18-*P. gingivalis* T22 coaggregation (Fig. 9). The Fab fragments from antisera raised against whole cells of *F. nucleatum* T18 and the 42-kDa OMP at 500 μg/ml inhibited coaggregation by 18.5 and 35.1%, respectively. At the same concentrations, the preimmune Fab fragments had no effect on coaggregation. The selective inhibition of coaggregation in the presence of the 42-kDa OMP-specific Fab fragments suggest that the 42-kDa OMP of *F. nucleatum* T18 is involved in mediating the adherence with *P. gingivalis* T22.

DISCUSSION

The *F. nucleatum-P. gingivalis* coaggregation represents a typical carbohydrate-lectin interaction; it is inhibited by lactose and lactose-related sugars and appears to be mediated by a carbohydrate receptor(s) on the *P. gingivalis* cells and a protein adhesin(s) on the *F. nucleatum* cells (16, 17). In this investigation, we have localized the adhesin activity of *F. nucleatum* T18 to the outer membrane. This conclusion is supported by the ability of *F. nucleatum* T18 vesicles and OMF to coaggregate with whole cells of *P. gingivalis* T22

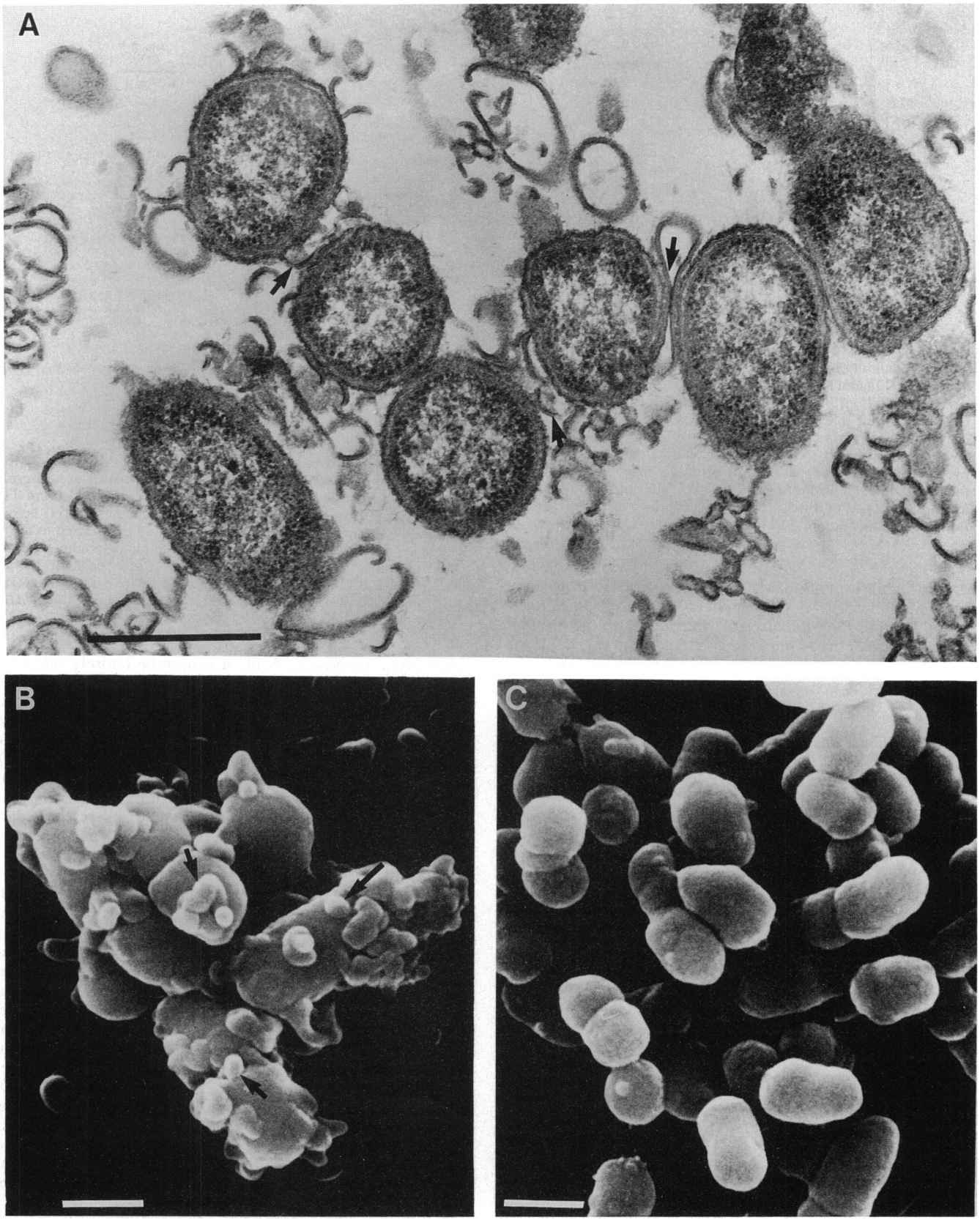

FIG. 3. Electron microscopy of coaggregates of *F. nucleatum* T18 OMF with *P. gingivalis* T22 cells. (A) Thin section through coaggregate of *F. nucleatum* T18 OMF with *P. gingivalis* T22 cells; arrows indicate membrane fractions interposed between whole cells of *P. gingivalis* T22. (B) Scanning micrograph of a coaggregate formed by *F. nucleatum* T18 OMF and *P. gingivalis* T22 cells; arrows indicate OMF structures. (C) Scanning micrograph of autoaggregate formed from *P. gingivalis* T22 cells. Note the relative lack of attached membranous structures compared with panel B. Bars, 0.5 μm.

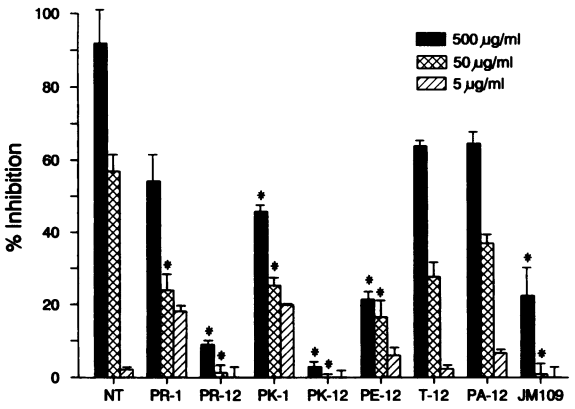

FIG. 4. Effect of proteolytic treatment of *F. nucleatum* T18 OMF on inhibition of coaggregation between whole cells of *F. nucleatum* T18 and *P. gingivalis* T22. The data are given as the mean percent inhibition, based on coaggregation without the addition of OMF (81.98% ± 0.85%), with the SD indicated by the bar. The data are from two experiments carried out in triplicate. *F. nucleatum* T18 OMF was untreated (NT) or treated with 1 mg of pronase (PR), proteinase K (PK), pepsin (PE), trypsin (T), or papain (PA) per ml for 1 or 12 h, as indicated. *E. coli* JM109 OMF (untreated) was used as a control. *, $P < 0.05$ versus coaggregation in the presence of untreated *F. nucleatum* T18 OMF (NT).

and the ability of the OMF of *F. nucleatum* T18 to selectively inhibit coaggregation between whole cells of *F. nucleatum* T18 and *P. gingivalis* T22. Furthermore, the proteinaceous nature of the *F. nucleatum* T18 adhesin was confirmed by the loss of coaggregation inhibition of the OMF after

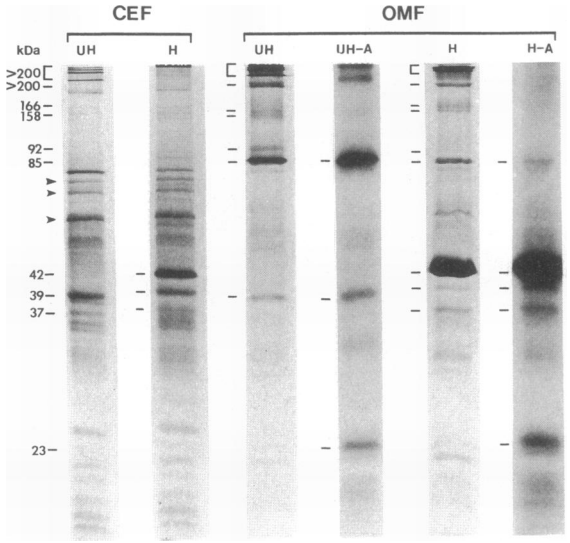

FIG. 5. SDS-PAGE analysis of *F. nucleatum* T18 CEF and OMF. *F. nucleatum* T18 CEF and OMF (40 μg of protein for gels, 50,000 cpm for autoradiographs) were run on SDS–12.5% PAGE gels, stained, and used for autoradiography as described in the text. Preparations of the CEF and OMF were unheated (UH) or heated (H) before electrophoresis as described in Materials and Methods. The corresponding autoradiographs (UH-A and H-A) are shown for the OMF preparations. The relative molecular sizes of proteins of interest are indicated on the left of the figure and by bars to the left of the individual lanes. Arrows indicate proteins that are selectively depleted in the OMF compared with the CEF.

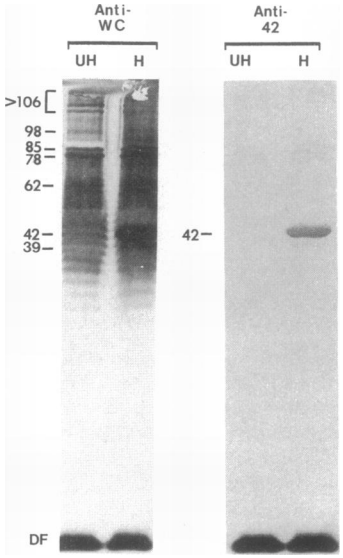

FIG. 6. Western blot of *F. nucleatum* T18 OMF probed with antiserum to *F. nucleatum* T18 whole cells (anti-WC) or antiserum to the *F. nucleatum* T18 42-kDa OMP (anti-42). *F. nucleatum* T18 OMF (40 μg of protein) was unheated (UH) or heated (H) before electrophoresis on SDS–12.5% PAGE gels and transferred to nitrocellulose. Blots were probed with the immunoglobulin-enriched ASC of antiserum to *F. nucleatum* T18 whole cells or the *F. nucleatum* T18 42-kDa OMP at 1:5,000. The relative molecular sizes (in kilodaltons) of proteins of interest are indicated on the left. DF, dye front.

proteolytic treatment. While it cannot be entirely ruled out that the adhesin activity of the OMF and vesicles was due to adhesins associated with proteinaceous appendages, it is unlikely, as neither fimbriae, pili, nor flagella have been reported for *F. nucleatum* (2, 25) and we have been unable to detect them on cells of *F. nucleatum* T18 (data not shown). In addition, the adhesin activity was not removed from the OMF by simple physical means, including sonication and shearing forces (data not shown). Taken together, these data indicate that the adherence observed is based on the activity of a surface-exposed protein adhesin located in the *F. nucleatum* T18 outer membrane.

A major OMP of *F. nucleatum* T18 with a mass of 42 kDa was found to be enriched in the coaggregation-inhibiting OMF. Immunogold studies with 42-kDa OMP-specific antibody indicated that the protein was localized to the bacterial cell envelope. This protein appears to correspond to the major OMP from other strains of *F. nucleatum*, reported as OMPs of 40 to 42 kDa, for which a number of properties have been described. Bakken and Jensen (2) examined the outer membranes of six strains of *F. nucleatum*, including ATCC 10953. They found a 40- to 42-kDa heat-modified major OMP in all but one strain, Fev1, in which the 42-kDa major OMP was present but not heat modified. Our studies revealed that the 42-kDa OMP of strain T18 was heat modified, and further characterization by two-dimensional SDS-PAGE demonstrated that the unheated protein migrated at 39, 85, 158, and >200 kDa. Antiserum raised to the heat-denatured 42-kDa OMP isolated from one-dimensional SDS-PAGE gels was found to react with the proteins originating at 39, 85, 158, and >200 kDa in Western blots of the two-dimensional SDS-PAGE (Fig. 7). The lack of reactivity of the 42-kDa OMP-specific antiserum with the non-heat-denatured proteins of 39, 85, 158, and >200 kDa in the

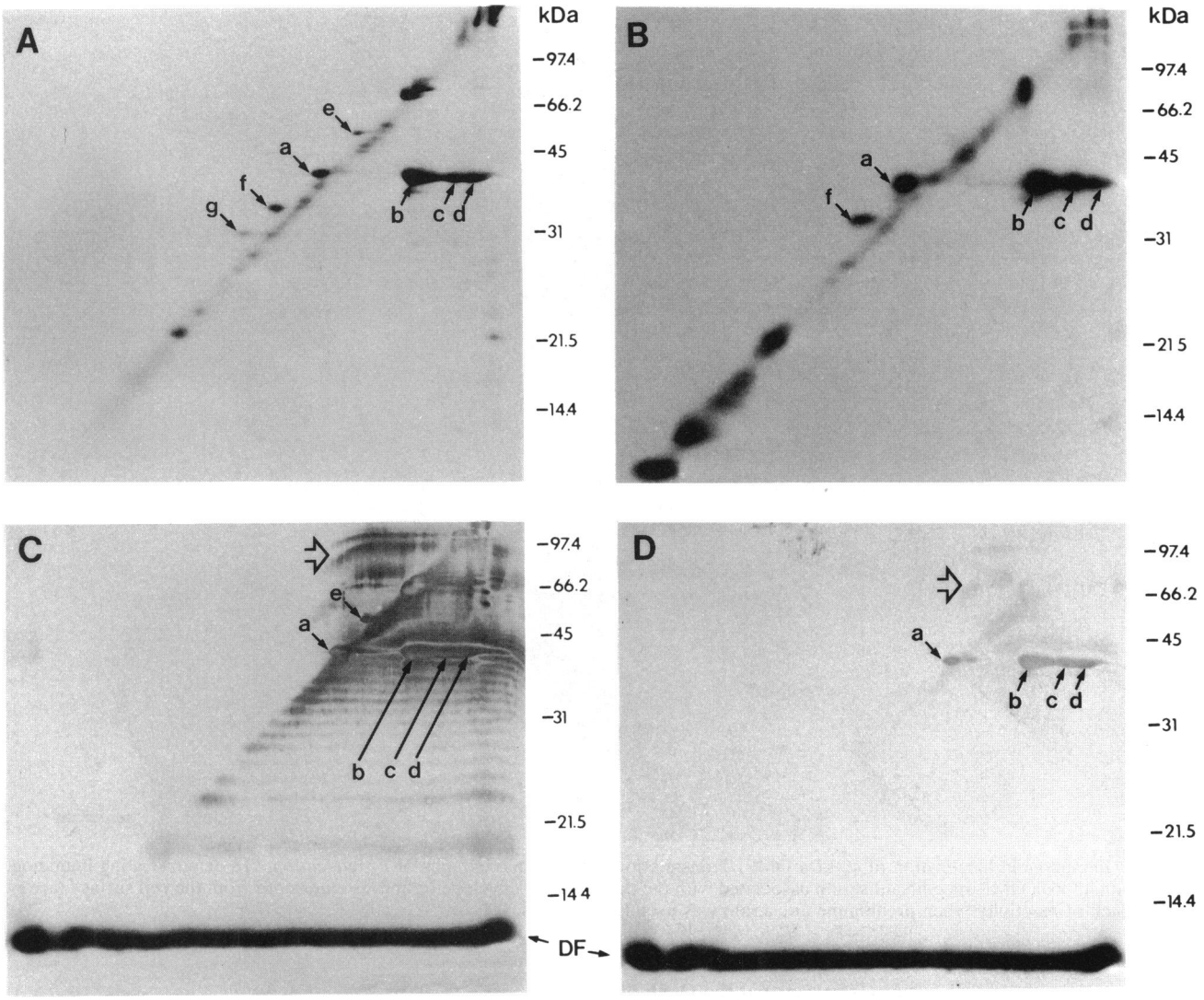

FIG. 7. Two-dimensional SDS-PAGE gels and Western blots of *F. nucleatum* T18 OMF. Gels were run as described in Materials and Methods. (A) Coomassie-stained gel, 100 μg of OMF (protein). (B) Autoradiograph of gel, 60 μg of OMF (protein). (C) Western blot of 100 μg (protein) of *F. nucleatum* T18 OMF probed with a 1:4,000 dilution of ASC of antiserum to *F. nucleatum* T18 whole cells. (D) Western blot of 100 μg (protein) of *F. nucleatum* T18 OMF probed with a 1:2,000 dilution of ASC of antiserum to *F. nucleatum* T18 42-kDa OMP. The heat-modified proteins are indicated with the letters a through g; the open arrows indicate reactivity thought to represent *F. nucleatum* T18 LPS. DF, dye front. Panel B is from reference 12.

one-dimensional SDS-PAGE gel (Fig. 6) suggests that the antiserum reacts primarily with heat-denatured epitopes. These findings are consistent with a monomeric polypeptide and complexes of the monomer; however, there is no evidence that the complex is composed of identical polypeptide units. Our studies additionally demonstrated that the 42-kDa protein from strain T18 was labeled when whole cells were extrinsically radiolabeled with ^{125}I, indicating that it was exposed on the bacterial cell surface. This is consistent with the findings of Bakken and Jensen (2), who also found that the major OMPs were associated with the peptidoglycan, suggesting that they span the outer membrane.

A 41-kDa major OMP (39 kDa in the unheated state) from *F. nucleatum* ATCC 10953, isolated by Takada and coworkers (32), was found to possess significant porin function as well as the immunobiological properties of B-cell mitogenicity, polyclonal B-cell activation, and enhanced migration of monocytes. N-terminal sequencing of the 41-kDa OMPs isolated from several strains of *F. nucleatum* revealed considerable similarity with a region in the C-terminal portion of the OmpA protein from *E. coli* and several other gram-negative species. Although the significance of this association is unclear, it is interesting that the OmpA protein is known to function as a bacteriophage receptor (8). Kaufman and DiRienzo (14) isolated what may be the same protein from *F. nucleatum* ATCC 10953 and demonstrated its probable role as an adhesin in mediating coaggregation between *F. nucleatum* ATCC 10953 and *Streptococcus sanguis* CC5A. The protein was isolated after cleavage of a trypsin-sensitive fragment, and the resulting 39.5-kDa protein was shown to specifically inhibit coaggregation.

The results of our studies suggest that the 42-kDa major OMP of *F. nucleatum* T18 was responsible, at least in part, for the coaggregation of this strain with *P. gingivalis* T22.

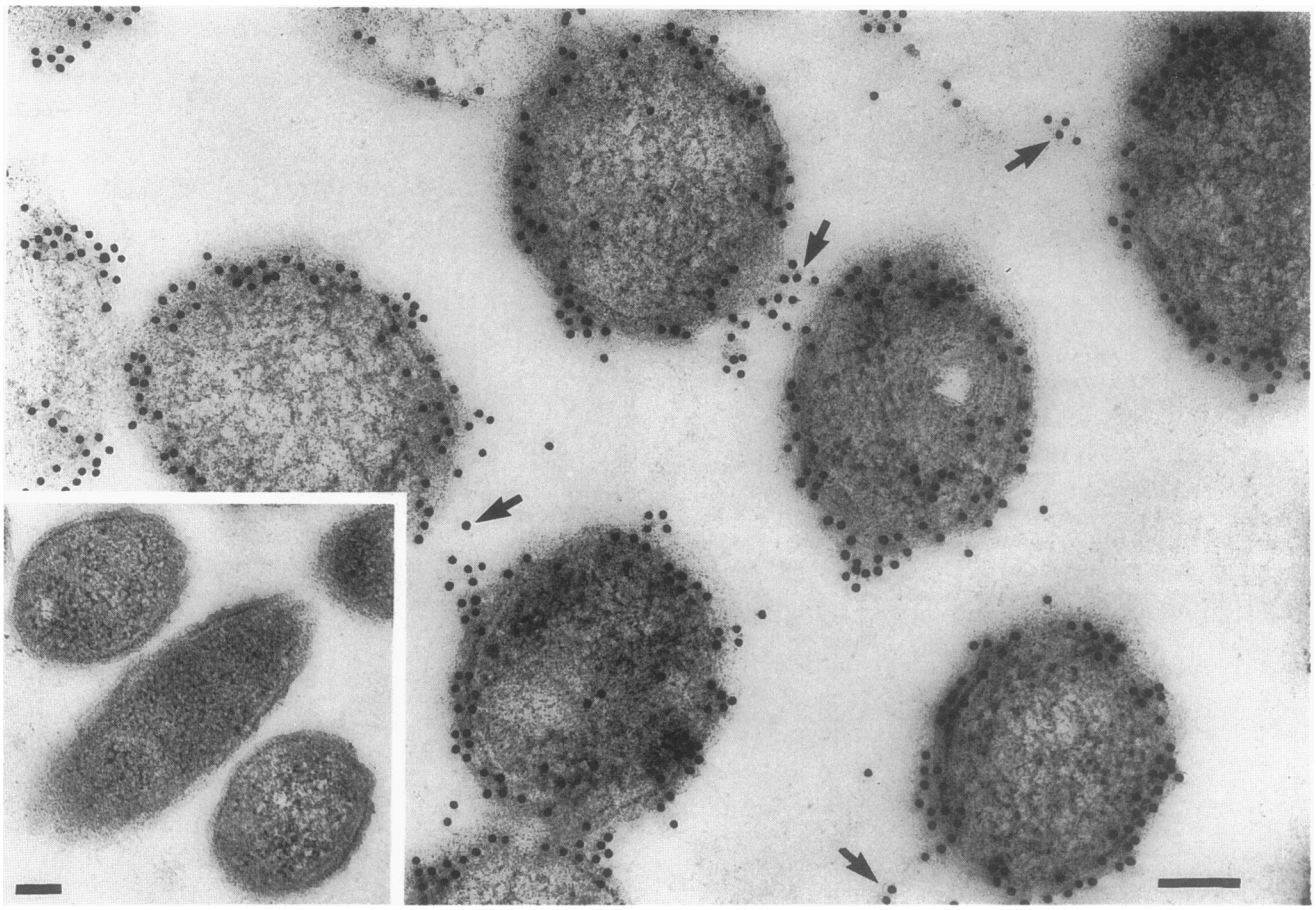

FIG. 8. Immunogold localization of 42-kDa OMP. Transmission electron micrographs of *F. nucleatum* T18 demonstrating immunogold labeling with 42-kDa OMP-specific antiserum associated with the bacterial cell envelope or fibrous extensions from the cell surface (arrows). Note the lack of reactivity when preimmune antiserum was used (inset). Bars, 0.1 μm.

Support for this includes the demonstration that the OMF of *F. nucleatum* T18 was enriched for both the 42-kDa OMP and adhesin activity and that Fab fragments from antiserum raised to the 42-kDa OMP specifically inhibited coaggregation. The fact that treatment of the *F. nucleatum* T18 cells with the 42-kDa OMP-specific Fab fragments resulted in a partial inhibition of coaggregation (35%; Fig. 9) is consistent

TABLE 1. Properties of *F. nucleatum* T18 membrane proteins[a]

Relative size of protein (kDa)	Selectively enriched in OMF	Heat modified	Surface labeled with ^{125}I	Reactive with whole-cell antiserum
>200	XX	XX	XX	XX[b]
166	X			
158	X	X	X	X
92	X	X		
85	X	X	X	X
78				X
62				X
42	X	X	X	X
39		X	X	X
37	X	X	X	
23			X	

[a] XX indicates more than one protein in the given size range.
[b] Size is >106 kDa on Western blots.

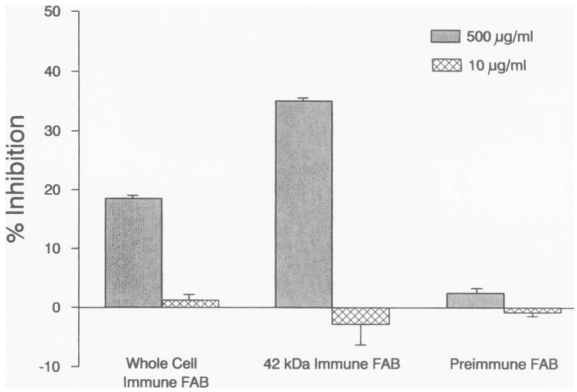

FIG. 9. Inhibition of coaggregation with Fab fragments. Purified Fab fragments from preimmune serum or immune antisera raised to *F. nucleatum* T18 whole cells and the *F. nucleatum* T18 42-kDa OMP were incorporated into the coaggregation assay at the indicated protein concentrations. The data are expressed as percent inhibition compared with controls to which no Fab fragments were added. Experiments were performed twice, once in triplicate and once in duplicate, for the immune Fab preparations, and once in duplicate for the preimmune Fab preparation. Level of coaggregation with whole cell and 42-kDa Fab fragments at 500 μg/ml versus controls, $P < 0.05$.

with previous data demonstrating a partial (80%) loss of coaggregation (16) after treatment of the *F. nucleatum* T18 cells with pronase. These data suggest several possibilities, including that the adhesin itself may be a multicomponent molecule, of which the 42-kDa OMP is only one part, or that multiple adhesins may be involved in mediating this interaction.

Examination of the 41-kDa major OMPs of *F. nucleatum* strains (1) by extrinsic radiolabeling and proteolytic digestion has suggested that a 3.5-kDa trypsin-sensitive fragment from the N terminus of the 41-kDa protein extends from the bacterial cell surface. Interestingly, the *F. nucleatum* ATCC 10953 adhesin involved in coaggregation with *S. sanguis* CC5A was found to be trypsin sensitive, whereas the adhesin of *F. nucleatum* T18 that is involved in coaggregation with *P. gingivalis* T22 is trypsin resistant. This suggests that although these coaggregations appear to be mediated at least in part by the same protein, the interactions most likely involve distinct domains, one resistant and one susceptible to trypsin treatment. This may be comparable to the properties that have been described for the 155-kDa OMP adhesin of *Capnocytophaga ochracea* ATCC 33596 (37). The coaggregation of this organism with *Streptococcus sanguis* H1 and *Actinomyces naeslundii* PK984 is rhamnose sensitive, while coaggregation with *Actinomyces israelii* PK16 is completely inhibited only by a combination of rhamnose and *N*-acetylneuraminic acid. Two classes of monoclonal antibody probes to *C. ochracea* have been identified: one completely blocks coaggregation with *S. sanguis* and *A. naeslundii* but only partially blocks coaggregation with *A. israelii*; the second completely blocks coaggregation with *S. sanguis*, partially blocks coaggregation with *A. naeslundii*, and has no effect on coaggregation with *A. israelii*. These results are consistent with earlier studies of coaggregation-defective mutants of *C. ochracea*, in which sequential loss of coaggregation with the three coaggregation partner strains was found (38). On this basis, it was proposed that the 155-kDa OMP adhesin of *C. ochracea* possesses two distinct rhamnose-sensitive activities (37). In the case of *F. nucleatum* coaggregation with *P. gingivalis* and *S. sanguis*, different regions of the 42-kDa OMP appear to be involved in coaggregation with the different partner strains. To further define the structure and function of the 42-kDa OMP of *F. nucleatum* T18, we are currently pursuing the isolation and purification of this protein at a molecular level.

ACKNOWLEDGMENTS

We thank D. Guerrero for his assistance with the electron microscopy, R. Wood for his help with the statistical analyses, and R. Borinski, T. Bramanti, W. Kennell, and A. Weinberg for discussions of this research. We also thank K. Hurst, V. Miller, and J. Pepe for their critical review of the manuscript.

This study was supported by Public Health Service grant DE-00212 from the National Institute of Dental Research and a grant from the University-Industry Cooperative Research Center at San Antonio. S.A.K. is a Physician-Scientist Awardee.

REFERENCES

1. **Bakken, V., S. Aaro, and H. B. Jensen.** 1989. Purification and partial characterization of a major outer-membrane protein of *Fusobacterium nucleatum*. J. Gen. Microbiol. **135:**3253–3262.
2. **Bakken, V., and H. B. Jensen.** 1986. Outer membrane proteins of *Fusobacterium nucleatum* Fev1. J. Gen. Microbiol. **132:** 1069–1078.
3. **Beachey, E. H., C. S. Giampapa, and S. N. Abraham.** 1988. Bacterial adherence: adhesin receptor-mediated attachment of pathogenic bacteria to mucosal surfaces. Am. Rev. Respir. Dis. **138:**S45–S48.
4. **Berryman, M. A., and R. D. Rodewald.** 1988. An enhanced method for post-embedding immunocytochemical staining that preserves cell membranes. J. Cell Biol. **107S:**111a.
5. **Bolton, A. E., and W. M. Hunter.** 1973. The labelling of proteins to high specific radioactivities by conjugation to a ^{125}I-containing acylating agent. Biochem. J. **133:**529–539.
6. **Borinski, R., and S. C. Holt.** 1990. Surface characteristics of *Wolinella recta* ATCC 33238 and human clinical isolates: correlation of structure with function. Infect. Immun. **58:**2770–2776.
7. **Brown, M. R. W., and P. Williams.** 1985. The influence of environment on envelope properties affecting survival of bacteria in infections. Annu. Rev. Microbiol. **39:**527–556.
8. **Datta, D. B., B. Arden, and U. Henning.** 1977. Major proteins of the *Escherichia coli* outer cell envelope membrane as bacteriophage receptors. J. Bacteriol. **131:**821–829.
9. **Ebersole, J. L., D. E. Frey, M. A. Taubman, and D. J. Smith.** 1980. An ELISA for measuring serum antibodies to *Actinobacillus actinomycetemcomitans*. J. Periodont. Res. **15:**621–632.
10. **Filip, C., G. Fletcher, J. L. Wulff, and C. F. Earhart.** 1973. Solubilization of the cytoplasmic membrane of *Escherichia coli* by the ionic detergent sodium-lauryl sarcosinate. J. Bacteriol. **115:**717–722.
11. **Gibbons, R. J.** 1989. Bacterial adhesion to oral tissues: a model for infectious diseases. J. Dent. Res. **68:**750–760.
12. **Holt, S. C., and T. E. Bramanti.** 1991. Factors in virulence expression and their role in periodontal disease pathogenesis. Crit. Rev. Oral Biol. Med. **2:**177–281.
13. **Holt, S. C., J. Ebersole, J. Felton, M. Brunsvold, and K. S. Kornman.** 1988. Implantation of *Bacteroides gingivalis* in nonhuman primates initiates progression of periodontitis. Science **239:**55–57.
14. **Kaufman, J., and J. M. DiRienzo.** 1989. Isolation of a corncob (coaggregation) receptor polypeptide from *Fusobacterium nucleatum*. Infect. Immun. **57:**331–337.
15. **Kennell, W., and S. C. Holt.** 1990. Comparative studies of the outer membranes of *Bacteroides gingivalis*, strains ATCC 33277, W50, W83, 381. Oral Microbiol. Immunol. **5:**121–130.
16. **Kinder, S., and S. C. Holt.** 1989. Characterization of coaggregation between *Bacteroides gingivalis* T22 and *Fusobacterium nucleatum* T18. Infect. Immun. **57:**3425–3433.
17. **Kolenbrander, P. E., and R. N. Andersen.** 1989. Inhibition of coaggregation between *Fusobacterium nucleatum* and *Porphyromonas gingivalis* by lactose and related sugars. Infect. Immun. **57:**3204–3209.
18. **Laemmli, U. K.** 1970. Cleavage of structural proteins during the assembly of the head of bacteriophage T4. Nature (London) **227:**680–685.
19. **Lantz, M. S., R. D. Allen, P. Bounelis, L. M. Switalski, and M. Hook.** 1990. *Bacteroides gingivalis* and *Bacteroides intermedius* recognize different sites on human fibrinogen. J. Bacteriol. **172:**716–726.
20. **Lantz, M. S., R. D. Allen, L. W. Duck, J. L. Blume, L. M. Switalski, and M. Hook.** 1991. Identification of *Porphyromonas gingivalis* components that mediate its interactions with fibronectin. J. Bacteriol. **173:**4263–4270.
21. **Macrina, F. L., M. T. Dertzbaugh, M. C. Halula, E. R. Krah III, and K. R. Jones.** 1990. Genetic approaches to the study of oral microflora: a review. Crit. Rev. Oral Biol. Med. **1:**207–227.
22. **Mayrand, D., and D. Grenier.** 1989. Biological activities of outer membrane vesicles. Can. J. Microbiol. **35:**607–613.
23. **McLean, I. W., and P. K. Nakane.** 1974. Periodate-lysine-paraformaldehyde fixative, a new fixative for immunoelectron microscopy. J. Histochem. Cytochem. **22:**1077–1083.
24. **Mergenhagen, S. E., A. L. Sandberg, B. M. Chassy, M. J. Brennan, M. K. Yeung, J. A. Donkersloot, and J. O. Cisar.** 1987. Molecular basis of bacterial adhesion in the oral cavity. Rev. Infect. Dis. **9**(Suppl. 5):S467–S474.
25. **Moore, W. E. C., L. V. Holdeman, and R. W. Kelley.** 1984. Genus II. *Fusobacterium Knorr* 1922, p. 631–637. *In* N. R. Krieg and J. G. Holt (ed.), Bergey's manual of systematic bacteriology, vol. 1. The Williams & Wilkins Co., Baltimore.

26. **Ofek, I., D. Zafriri, J. Goldhar, and B. I. Eisenstein.** 1990. Inability of toxin inhibitors to neutralize enhanced toxicity caused by bacteria adherent to tissue culture cells. Infect. Immun. **58**:3737–3742.
27. **Reynolds, E. S.** 1963. The use of lead citrate at high pH as an electron-opaque stain in electron microscopy. J. Cell Biol. **17**:208–212.
28. **Sambrook, J., E. F. Fritsch, and T. Maniatis.** 1989. Molecular cloning: a laboratory manual, 2nd ed. Cold Spring Harbor Laboratory, Cold Spring Harbor, N.Y.
29. **Slots, J., and R. J. Gibbons.** 1978. Attachment of *Bacteroides melaninogenicus* subsp. *asaccharolyticus* to oral surfaces and its possible role in colonization of the mouth and of periodontal pockets. Infect. Immun. **19**:254–264.
30. **Svanborg Eden, C., L. Hagberg, L. A. Hanson, S. Hull, U. Jodal, H. Leffler, H. Lomberg, and E. Straube.** 1983. Bacterial adherence—a pathogenic mechanism in urinary tract infections caused by *Escherichia coli*. Prog. Allergy **33**:175–188.
31. **Svanborg Eden, C., S. Hausson, U. Jodal, G. Lidin-Janson, K. Lincoln, H. Linder, H. Lomberg, P. De Man, S. Marild, J. Martinell, K. Plos, T. Sandberg, and K. Stenqvist.** 1988. Host-parasite interaction in the urinary tract. J. Infect. Dis. **157**:421–426.
32. **Takada, H., T. Ogawa, F. Yoshimura, K. Otsuka, S. Kokeguchi, K. Kato, T. Umemoto, and S. Kotani.** 1988. Immunobiological activities of a porin fraction isolated from *Fusobacterium nucleatum* ATCC 10953. Infect. Immun. **56**:855–863.
33. **Tanner, A. C. R., C. Haffer, G. T. Bratthall, R. A. Visconti, and S. S. Socransky.** 1979. A study of the bacteria associated with advancing periodontitis in man. J. Clin. Periodontol. **6**:278–307.
34. **Towbin, H., T. Staehelin, and J. Gordon.** 1979. Electrophoretic transfer of proteins from polyacrylamide gels to nitrocellulose sheets: procedure and some applications. Proc. Natl. Acad. Sci. USA **76**:4350–4354.
35. **Weinberg, A., and S. C. Holt.** 1990. Interaction of *Treponema denticola* TD-4, GM-1, and MS25 with human gingival fibroblasts. Infect. Immun. **58**:1720–1729.
36. **Weinberg, A., and S. C. Holt.** 1991. Chemical and biological activities of a 64-kilodalton outer sheath protein from *Treponema denticola* strains. J. Bacteriol. **173**:6935–6947.
37. **Weiss, E. I., I. Eli, B. Shenitzki, and N. Smorodinsky.** 1990. Identification of the rhamnose-sensitive adhesin of *Capnocytophaga ochracea* ATCC 33596. Arch. Oral Biol. **35**:127S–130S.
38. **Weiss, E. I., J. London, P. E. Kolenbrander, A. S. Kagermeier, and R. N. Andersen.** 1987. Characterization of lectinlike surface components on *Capnocytophaga ochracea* ATCC 33596 that mediate coaggregation with gram-positive oral bacteria. Infect. Immun. **55**:1198–1202.
39. **Whitnack, E., and E. H. Beachey.** 1982. Antiopsonic activity of fibrinogen bound to M protein on the surface of group A streptococci. J. Clin. Invest. **69**:1042–1045.
40. **Zambon, J. J., H. S. Reynolds, and J. Slots.** 1981. Black-pigmented *Bacteroides* spp. in the human oral cavity. Infect. Immun. **32**:198–203.